Nonlinear Model Predictive Control for Disturbance Rejection in Isoenergetic-isochoric Flash Processes

Ritschel, Tobias K. S.; Jørgensen, John Bagterp

Published in:
IFAC-PapersOnLine

Link to article, DOI:
10.1016/j.ifacol.2019.06.159

Publication date:
2019

Document Version
Publisher's PDF, also known as Version of record

Available online at www.sciencedirect.com

ScienceDirect

IFAC Papers Online CONFERENCE PAPER ARCHIVE

IFAC PapersOnLine 52-1 (2019) 796–801

Nonlinear Model Predictive Control for Disturbance Rejection in Isoenergetic-isochoric Flash Processes ⋆

Tobias K. S. Ritschel, John Bagterp Jørgensen

Department of Applied Mathematics and Computer Science & Center for Energy Resources Engineering (CERE), Technical University of Denmark, DK-2800 Kgs. Lyngby, Denmark

Abstract: We present a nonlinear model predictive control (NMPC) algorithm for semi-explicit index-1 stochastic differential-algebraic equations. It is natural to model isoenergetic-isochoric (constant energy-constant volume) flash processes with such equations. The algorithm uses the continuous-discrete extended Kalman filter (EKF) for state estimation, and it uses a single-shooting method to solve the involved optimal control problems. It computes the gradients with an adjoint method. The isoenergetic-isochoric flash is also called the UV flash, and it is important to rigorous models of phase equilibrium processes because it is a mathematical statement of the second law of thermodynamics. NMPC algorithms for UV flash processes are therefore relevant to both safe and economical operation of phase equilibrium processes such as flash separation, distillation, two-phase flow in pipes, and oil production. We design the NMPC algorithm for disturbance rejection, and we therefore augment the state vector with the unknown disturbance variables in the continuous-discrete EKF. We present a numerical example of economical NMPC of a UV flash separation process. It involves output constraints and the estimation of an unknown and unmeasured disturbance. The computation time of the NMPC algorithm does not exceed 3.14 s in any of the 5 min control intervals. This indicates that real-time NMPC of UV flash separation processes is computationally feasible.

Keywords: Nonlinear model predictive control, The extended Kalman filter, Single-shooting, Disturbance rejection, Vapor-liquid equilibrium, Differential-algebraic equations

1. INTRODUCTION

Nonlinear model predictive control (NMPC) algorithms compute a closed-loop feedback control strategy using the moving horizon optimization principle, i.e. by solving a sequence of open-loop optimal control problems (OCPs) (Binder et al., 2001). The objective of NMPC algorithms is either to optimize the economics of the process or to minimize the distance to predefined setpoints. NMPC algorithms are used to control a variety of chemical processes including stirred tank reactors, batch reactors, fermentors, distillation columns, and production from oil reservoirs.

Chemical processes often involve thermodynamic equilibrium between phases. The phase equilibrium conditions are derived from the second law of thermodynamics, i.e. the entropy of a closed system in equilibrium is maximal. The isoenergetic-isochoric (constant energy-constant volume) flash is a mathematical statement of the second law of thermodynamics and is therefore key to rigorous modeling of phase equilibrium processes. The isoenergetic-isochoric flash is also called the UV (or UVn) flash because it involves constraints on the internal energy, U, the volume, V, and the total mixture composition (in moles), n. The solution to the UV flash is the equilibrium temperature, pressure, and phase compositions which maximize the entropy subject to these constraints. Therefore, the UV flash can be formulated as an equality-constrained optimization problem (Michelsen, 1999). The phase equilibrium conditions are the corresponding first-order optimality conditions which are a set of algebraic equations. Consequently, it is natural to model dynamic UV flash processes with differential-algebraic equations (DAEs). The UV flash has been used in models of flash separation (Castier, 2010; Arendsen and Versteeg, 2009; Lima et al., 2008), distillation (Flatby et al., 1994), and computational fluid dynamical processes (Hammer and Morin, 2014; Qiu et al., 2014). Furthermore, algorithms for dynamic optimization and state estimation of UV flash processes have been considered recently (Ritschel and Jørgensen, 2018; Ritschel et al., 2018). However, NMPC of UV flash processes has not yet been addressed.

NMPC algorithms combine state estimation algorithms with dynamic optimization algorithms. The extended Kalman filter (EKF) is commonly used for state estimation of nonlinear processes (Mobed et al., 2017; Jørgensen et al., 2007). Alternatives include the unscented Kalman filter and particle filters (Simon, 2006) as well as the ensemble Kalman filter (Evensen, 2009a,b), moving-horizon estimation (Alessandri et al., 2010), and neural network-based algorithms (Talebi et al., 2010). OCPs are often solved with direct methods (Binder et al., 2001), i.e. single-shooting, multiple-shooting, or simultaneous collocation.

⋆ This project is funded by Innovation Fund Denmark in the OPTION project (63-2013-3).

10.1016/j.ifacol.2019.06.159

Computationally efficient implementation of such methods requires the evaluation of gradients. The gradients can be computed with an adjoint method (Jørgensen, 2007) or with a forward method (Kristensen et al., 2004) in the single- and multiple-shooting approaches. NMPC algorithms for disturbance rejection either 1) estimate the disturbance variables (Vatankhah and Farrokhi, 2017; Morari and Maeder, 2012; Huang et al., 2010) or 2) represent the uncertainty in the disturbance variables with a scenario-tree (Subramanian et al., 2015).

In this work, we present an NMPC algorithm for disturbance rejection in UV flash processes. The algorithm combines the continuous-discrete EKF with single-shooting and an adjoint method for computing gradients. We model the UV flash processes with semi-explicit index-1 stochastic DAEs. We augment the states with the disturbance variables and exploit the structure of the augmented DAE system to improve computational performance. We use the open-source thermodynamic software ThermoLib (Ritschel et al., 2017, 2016) to evaluate thermodynamic functions. It is tailored for computation of first and second order derivatives which are needed for efficient implementation of the single-shooting method and in the adjoint method. We present a numerical example of output-constrained economical NMPC of a UV flash separation process that involves an unknown and unmeasured disturbance.

This paper is structured as follows. We describe the semi-explicit index-1 stochastic DAE system in Section 2, and we discuss the numerical simulation of such systems in Section 3. In Section 4, we discuss the estimation of the states and disturbance variables with the continuous-discrete EKF. We describe the open-loop OCP and the single-shooting method in Section 5. We describe the flash separation process in Section 6, and we present the numerical example in Section 7. Conclusions are given in Section 8.

2. SEMI-EXPLICIT INDEX-1 STOCHASTIC DIFFERENTIAL-ALGEBRAIC EQUATIONS

We consider stochastic DAEs that are in the form

$$G(\boldsymbol{x}(t), \boldsymbol{y}(t), \boldsymbol{z}(t)) = 0, \tag{1a}$$
$$d\boldsymbol{x}(t) = F(\boldsymbol{y}(t), u(t), d(t))dt + \sigma(\boldsymbol{y}(t), u(t), d(t))d\boldsymbol{\omega}(t). \tag{1b}$$

$\boldsymbol{x}(t)$, $\boldsymbol{y}(t)$, and $\boldsymbol{z}(t)$ are vectors of state variables, algebraic variables, and adjoint algebraic variables, respectively. The algebraic equations (1a) represent phase equilibrium conditions, and the stochastic differential equations (1b) represent conservation equations. $u(t)$ are the manipulated inputs, and $d(t)$ are the disturbance variables. The initial states are normally distributed, i.e. $\boldsymbol{x}(t_0) \sim N(x_0, P_0)$. $\boldsymbol{\omega}(t)$ is a standard Wiener process, i.e. it has an incremental covariance of Idt. The algebraic equations (1a) are of index 1 for the processes that we consider. Therefore, they can be solved for $\boldsymbol{y}(t)$ and $\boldsymbol{z}(t)$ when $\boldsymbol{x}(t)$ is given. The measurements, $\boldsymbol{y}^m(t_k)$, of the outputs, $\boldsymbol{z}^m(t_k)$, are obtained at discrete times, t_k:

$$\boldsymbol{z}^m(t_k) = H(\boldsymbol{y}(t_k)), \tag{2a}$$
$$\boldsymbol{y}^m(t_k) = \boldsymbol{z}^m(t_k) + \boldsymbol{v}(t_k). \tag{2b}$$

$\boldsymbol{v}_k = \boldsymbol{v}(t_k)$ is the measurement noise. It is normally distributed, i.e. $\boldsymbol{v}_k \sim N(0, T_k)$.

3. NUMERICAL SIMULATION

We discretize the stochastic DAE (1) with a semi-implicit scheme, i.e. we discretize the drift and the diffusion terms in (1b) with Euler's implicit and explicit method, respectively. Between measurement k and $k+1$, we compute N_k time steps. In each time step, we solve $R_{k,n+1} = 0$ for $w_{k,n+1} = [x_{k,n+1}; y_{k,n+1}; z_{k,n+1}]$ where

$$\begin{aligned} R_{k,n+1} &= R_{k,n+1}(w_{k,n+1}; x_{k,n}, y_{k,n}, u_k, d_k) \\ &= R_{k,n+1}(x_{k,n+1}, y_{k,n+1}, z_{k,n+1}; x_{k,n}, y_{k,n}, u_k, d_k) \\ &= \begin{bmatrix} D_{k,n+1}(x_{k,n+1}, y_{k,n+1}; x_{k,n}, y_{k,n}, u_k, d_k) \\ G(x_{k,n+1}, y_{k,n+1}, z_{k,n+1}) \end{bmatrix}. \end{aligned} \tag{3}$$

The discretized stochastic differential equations are

$$\begin{aligned} D_{k,n+1} &= D_{k,n+1}(x_{k,n+1}, y_{k,n+1}; x_{k,n}, y_{k,n}, u_k, d_k) \\ &= x_{k,n+1} - F(y_{k,n+1}, u_k, d_k)\Delta t_{k,n} \\ &\quad - \sigma(y_{k,n}, u_k, d_k)\Delta\omega_{k,n} - x_{k,n}. \end{aligned} \tag{4}$$

We sample the increments, $\Delta\omega_{k,n}$, from $N(0, \mathrm{I}\Delta t_{k,n})$. We solve $R_{k,n+1} = 0$ with an inexact Newton method:

$$w^{l+1}_{k,n+1} = w^l_{k,n+1} + \Delta w^l_{k,n+1}. \tag{5}$$

In each Newton iteration, we solve

$$M\Delta w^l_{k,n+1} = -R_{k,n+1}(w^l_{k,n+1}), \tag{6}$$

for the Newton step. The iteration matrix, M, is

$$M \approx \frac{\partial R_{k,n+1}}{\partial w_{k,n+1}} = \begin{bmatrix} \mathrm{I} & -\dfrac{\partial F}{\partial y}\Delta t_{k,n} & 0 \\ \dfrac{\partial G}{\partial x} & \dfrac{\partial G}{\partial y} & \dfrac{\partial G}{\partial z} \end{bmatrix}. \tag{7}$$

4. STATE AND DISTURBANCE ESTIMATION

In order to estimate the disturbances, we augment the stochastic DAE system (1) with a stochastic differential equation for the disturbance variables:

$$G(\boldsymbol{x}(t), \boldsymbol{y}(t), \boldsymbol{z}(t)) = 0, \tag{8a}$$
$$d\boldsymbol{x}(t) = F(\boldsymbol{y}(t), u(t), \boldsymbol{d}(t))dt + \sigma(\boldsymbol{y}(t), u(t), \boldsymbol{d}(t))d\boldsymbol{\omega}(t), \tag{8b}$$
$$d\boldsymbol{d}(t) = \sigma_d d\boldsymbol{\omega}_d(t). \tag{8c}$$

The measurement equations (2) remain unchanged. We use σ_d to tune the filter. We initialize the continuous-discrete EKF with $\hat{x}_{0|-1} = x_0$, $\hat{d}_{0|-1} = d_0$, $P^{xx}_{0|-1} = P^{xx}_0$, $P^{dx}_{0|-1} = 0$, and $P^{dd}_{0|-1} = P^{dd}_0$. d_0 is an initial estimate of the disturbance variables. We use P^{dd}_0 for tuning of the filter.

4.1 Measurement-update

The one-step ahead prediction of the measurements, $\hat{y}^m_{k|k-1}$, and its approximate covariance, $T_{k|k-1}$, are

$$\hat{y}^m_{k|k-1} = H(\hat{y}_{k|k-1}), \tag{9a}$$
$$T_{k|k-1} = C_k P^{xx}_{k|k-1} C'_k + T_k, \tag{9b}$$

where

$$C_k = \frac{\partial H}{\partial y}(\hat{y}_{k|k-1})\frac{\partial \hat{y}_{k|k-1}}{\partial \hat{x}_{k|k-1}}. \tag{10}$$

The sensitivities, $\frac{\partial \hat{y}_{k|k-1}}{\partial \hat{x}_{k|k-1}}$ and $\frac{\partial \hat{z}_{k|k-1}}{\partial \hat{x}_{k|k-1}}$, satisfy

$$\begin{bmatrix} \frac{\partial G}{\partial y} & \frac{\partial G}{\partial z} \end{bmatrix} \begin{bmatrix} \frac{\partial \hat{y}_{k|k-1}}{\partial \hat{x}_{k|k-1}} \\ \frac{\partial \hat{z}_{k|k-1}}{\partial \hat{x}_{k|k-1}} \end{bmatrix} = -\frac{\partial G}{\partial x}. \tag{11}$$

The innovation error is

$$e_k = y_k^m - \hat{y}_{k|k-1}^m, \tag{12}$$

and the Kalman filter gain matrices are

$$K_{fx,k} = P_{k|k-1}^{xx} C_k' T_{k|k-1}^{-1}, \tag{13a}$$
$$K_{fd,k} = P_{k|k-1}^{dx} C_k' T_{k|k-1}^{-1}. \tag{13b}$$

The filtered estimates of the states and disturbance variables and their covariance matrices are

$$\hat{x}_{k|k} = \hat{x}_{k|k-1} + K_{fx,k} e_k, \tag{14a}$$
$$\hat{d}_{k|k} = \hat{d}_{k|k-1} + K_{fd,k} e_k, \tag{14b}$$
$$P_{k|k}^{xx} = P_{k|k-1}^{xx} - K_{fx,k} T_{k|k-1} K_{fx,k}', \tag{14c}$$
$$P_{k|k}^{dx} = P_{k|k-1}^{dx} - K_{fd,k} T_{k|k-1} K_{fx,k}', \tag{14d}$$
$$P_{k|k}^{dd} = P_{k|k-1}^{dd} - K_{fd,k} T_{k|k-1} K_{fd,k}'. \tag{14e}$$

4.2 Time-update

We compute the one-step ahead predictions at time t_{k+1} by solving

$$\hat{x}_k(t_k) = \hat{x}_{k|k}, \tag{15a}$$
$$G(\hat{x}_k(t), \hat{y}_k(t), \hat{z}_k(t)) = 0, \qquad t \in [t_k; t_{k+1}], \tag{15b}$$
$$d\hat{x}_k(t) = F(\hat{y}_k(t), u(t), \hat{d}_k(t))dt, \quad t \in [t_k; t_{k+1}], \tag{15c}$$

where $u(t) = u_{k|k}$ and $\hat{d}_k(t) = \hat{d}_{k|k}$. In order to compute the one-step ahead predictions of the covariance matrices, we compute the sensitivities, $\Phi_{xx}(t,s) = \frac{\partial \hat{x}_k(t)}{\partial \hat{x}_k(s)}$, $\Phi_{yx}(t,s) = \frac{\partial \hat{y}_k(t)}{\partial \hat{x}_k(s)}$, $\Phi_{zx}(t,s) = \frac{\partial \hat{z}_k(t)}{\partial \hat{x}_k(s)}$, $\Phi_{xd}(t,s) = \frac{\partial \hat{x}_k(t)}{\partial \hat{d}_k(s)}$, $\Phi_{yd}(t,s) = \frac{\partial \hat{y}_k(t)}{\partial \hat{d}_k(s)}$, and $\Phi_{zd}(t,s) = \frac{\partial \hat{z}_k(t)}{\partial \hat{d}_k(s)}$, by solving

$$\frac{\partial G}{\partial x}\Phi_{xx}(t,s) + \frac{\partial G}{\partial y}\Phi_{yx}(t,s) + \frac{\partial G}{\partial z}\Phi_{zx}(t,s) = 0, \tag{16a}$$
$$\frac{\partial G}{\partial x}\Phi_{xd}(t,s) + \frac{\partial G}{\partial y}\Phi_{yd}(t,s) + \frac{\partial G}{\partial z}\Phi_{zd}(t,s) = 0, \tag{16b}$$
$$\frac{d\Phi_{xx}(t,s)}{dt} = \frac{\partial F}{\partial y}\Phi_{yx}(t,s), \tag{16c}$$
$$\frac{d\Phi_{xd}(t,s)}{dt} = \frac{\partial F}{\partial y}\Phi_{yd}(t,s) + \frac{\partial F}{\partial d}\Phi_{dd}(t,s), \tag{16d}$$

where $\Phi_{xx}(s,s) = \mathrm{I}$, $\Phi_{xd}(s,s) = 0$, and $\Phi_{dd}(t,s) = \mathrm{I}$. The covariance matrices are given by (Jørgensen et al., 2007)

$$\begin{aligned} P_k^{xx}(t) = {} & \Phi_{xx} P_{k|k}^{xx} \Phi_{xx}' + \Phi_{xd} P_{k|k}^{dx} \Phi_{xx}' \\ & + \Phi_{xx} (P_{k|k}^{dx})' \Phi_{xd}' + \Phi_{xd} P_{k|k}^{dd} \Phi_{xd}' \\ & + \int_{t_k}^{t} \Omega_{xx}(t,s)\Omega_{xx}(t,s)' + \Omega_{xd}(t,s)\Omega_{xd}(t,s)' ds, \end{aligned} \tag{17a}$$

$$\begin{aligned} P_k^{dx}(t) = {} & \Phi_{dd} P_{k|k}^{dx} \Phi_{xx}' + \Phi_{dd} P_{k|k}^{dd} \Phi_{xd}' \\ & + \int_{t_k}^{t} \Omega_{dd}(t,s)\Omega_{xd}(t,s)' ds, \end{aligned} \tag{17b}$$

$$P_k^{dd}(t) = \Phi_{dd} P_{k|k}^{dd} \Phi_{dd}' + \int_{t_k}^{t} \Omega_{dd}(t,s)\Omega_{dd}(t,s)' ds, \tag{17c}$$

where the sensitivity matrices are evaluated at t and t_k, e.g. $\Phi_{xx} = \Phi_{xx}(t, t_k)$, and

$$\Omega_{xx}(t,s) = \Phi_{xx}(t,s)\sigma(\hat{y}_k(s), u(s), \hat{d}_k(s)), \tag{18a}$$
$$\Omega_{xd}(t,s) = \Phi_{xd}(t,s)\sigma_d, \tag{18b}$$
$$\Omega_{dd}(t,s) = \Phi_{dd}(t,s)\sigma_d. \tag{18c}$$

4.3 Numerical solution of the time-update equations

We solve the time-update equations (15) with Euler's implicit method, i.e. we solve the equations

$$\begin{bmatrix} D_{k,n+1}(\hat{x}_{k,n+1}, \hat{y}_{k,n+1}; \hat{x}_{k,n}, u_{k|k}, \hat{d}_{k|k}) \\ G(\hat{x}_{k,n+1}, \hat{y}_{k,n+1}, \hat{z}_{k,n+1}) \end{bmatrix} = 0, \tag{19}$$

where the discretized differential equations are

$$D_{k,n+1} = \hat{x}_{k,n+1} - F(\hat{y}_{k,n+1}, u_{k|k}, \hat{d}_{k|k})\Delta t_{k,n} - \hat{x}_{k,n}. \tag{20}$$

The sensitivities satisfy

$$\begin{bmatrix} \mathrm{I} & -\frac{\partial F}{\partial y}\Delta t_{k,n} & 0 \\ \frac{\partial G}{\partial x} & \frac{\partial G}{\partial y} & \frac{\partial G}{\partial z} \end{bmatrix} \begin{bmatrix} \Phi_{xx} & \Phi_{xd} \\ \Phi_{yx} & \Phi_{yd} \\ \Phi_{zx} & \Phi_{zd} \end{bmatrix} = \begin{bmatrix} \mathrm{I} & \frac{\partial F}{\partial d}\Delta t_{k,n} \\ 0 & 0 \end{bmatrix}, \tag{21}$$

where the sensitivity matrices are evaluated at $t_{k,n+1}$ and $t_{k,n}$, e.g. $\Phi_{xx} = \Phi_{xx}(t_{k,n+1}, t_{k,n})$. We discretize the integrals in (17) with a right rectangle quadrature rule:

$$\begin{aligned} P_{k,n+1}^{xx} = {} & \Phi_{xx} P_{k,n}^{xx} \Phi_{xx}' + \Phi_{xd} P_{k,n}^{dx} \Phi_{xx}' + \Phi_{xx} (P_{k,n}^{dx})' \Phi_{xd}' \\ & + \Phi_{xd} P_{k,n}^{dd} \Phi_{xd}' + (\Omega_{xx}\Omega_{xx}' + \Omega_{xd}\Omega_{xd}')\,\Delta t_{k,n}, \end{aligned} \tag{22a}$$

$$P_{k,n+1}^{dx} = P_{k,n}^{dx} \Phi_{xx}' + P_{k,n}^{dd} \Phi_{xd}' + \Omega_{dd}\Omega_{xd}' \Delta t_{k,n}, \tag{22b}$$
$$P_{k,n+1}^{dd} = P_{k,n}^{dd} + \Omega_{dd}\Omega_{dd}' \Delta t_{k,n}. \tag{22c}$$

The sensitivities and the matrices Ω_{xx}, Ω_{xd}, and Ω_{dd}, in (22) are evaluated at $t_{k,n+1}$ and $t_{k,n}$. The sensitivity matrices in (22) are therefore the ones that we solve (21) for. We have exploited that $\Phi_{dd}(t,s) = \mathrm{I}$ in (21) and (22).

5. DYNAMIC OPTIMIZATION

We assume that there is one control interval in between measurements. At sample time t_k, we solve the OCP

$$\min_{[x(t);y(t);z(t)]_{t_k}^{t_{k+N_h}}, \{u_{j|k}\}_{j=k}^{k+N_h-1}} \phi\left([y(t); u(t); d(t)]_{t_k}^{t_{k+N_h}}\right), \tag{23a}$$

subject to

$$x(t_k) = \hat{x}_{k|k}, \tag{23b}$$
$$G(x(t), y(t), z(t)) = 0, \qquad t \in [t_k, t_{k+N_h}], \tag{23c}$$
$$\dot{x}(t) = F(y(t), u(t), d(t)), \ t \in [t_k, t_{k+N_h}], \tag{23d}$$
$$u(t) = u_{j|k}, \ t \in [t_j, \ t_{j+1}[, \ j = k, \ldots, k+N_h-1, \tag{23e}$$
$$d(t) = \hat{d}_{j|k}, \ t \in [t_j, \ t_{j+1}[, \ j = k, \ldots, k+N_h-1, \tag{23f}$$
$$\{u_{j|k}\}_{j=k}^{k+N_h-1} \in \mathcal{U}, \tag{23g}$$

where the objective function, ϕ, is in Lagrange form:

$$\phi\left([y(t); u(t); d(t)]_{t_k}^{t_{k+N_h}}\right) = \int_{t_k}^{t_{k+N_h}} \Phi(y(t), u(t), d(t))dt. \tag{24}$$

We consider a control and prediction horizon of N_h control intervals. $[x(t); y(t); z(t)]_{t_k}^{t_{k+N_h}}$ is a vector of dependent

optimization variables, and $\{u_{j|k}\}_{j=k}^{k+N_h-1}$ are independent optimization variables. The DAE system (23c)-(23d) is deterministic, i.e. there is no process noise. (23e)-(23f) are zero-order-hold parametrizations of the manipulated inputs and the disturbance variables, and (23g) are constraints on the manipulated inputs. We assume that $\hat{d}_{j|k} = \hat{d}_{k|k}$ for $j = k+1, \ldots, k+N_h-1$. The OCP (23) needs the current estimates of the states, $\hat{x}_{k|k}$, and disturbance variables, $\hat{d}_{k|k}$. They are computed by the continuous-discrete EKF.

5.1 Single-shooting

We use the single-shooting algorithm described by Ritschel et al. (2018) to solve the OCP (23). We define the objective function, ψ, as

$$\begin{aligned}\psi &= \psi(\{u_{j|k}\}_{j=k}^{k+N_h-1}; \hat{x}_{k|k}, \{\hat{d}_{j|k}\}_{j=k}^{k+N_h-1}) \\ &= \left\{ \phi : \text{ (23b)-(23f) } \right\}. \end{aligned} \tag{25}$$

That is, ψ is the objective function ϕ in (24) evaluated using the solution of the DAE system (23c)-(23d) with the initial condition (23b) and the zero-order-hold parametrizations of the manipulated inputs and the disturbance variables (23e)-(23f). In the single-shooting approach, we solve the finite dimensional nonlinear program

$$\min_{\{u_{j|k}\}_{j=k}^{k+N_h-1}} \quad \psi = \psi(\{u_{j|k}\}_{j=k}^{k+N_h-1}; \hat{x}_{k|k}, \{\hat{d}_{j|k}\}_{j=k}^{k+N_h-1}), \tag{26a}$$

$$\text{s.t.} \qquad \{u_{j|k}\}_{j=k}^{k+N_h-1} \in \mathcal{U}. \tag{26b}$$

We solve the DAE system (23c)-(23d) with Euler's implicit method. For each time step, we solve the residual equations, $R_{j,n+1} = 0$, for $w_{j,n+1}$ where

$$\begin{aligned} R_{j,n+1} &= R_{j,n+1}(w_{j,n+1}; x_{j,n}, u_{j|k}, \hat{d}_{j|k}) \\ &= R_{j,n+1}(x_{j,n+1}, y_{j,n+1}, z_{j,n+1}; x_{j,n}, u_{j|k}, \hat{d}_{j|k}) \\ &= \begin{bmatrix} D_{j,n+1}(x_{j,n+1}, y_{j,n+1}; x_{j,n}, u_{j|k}, \hat{d}_{j|k}) \\ G(x_{j,n+1}, y_{j,n+1}, z_{j,n+1}) \end{bmatrix}, \end{aligned} \tag{27}$$

and the discretized differential equations are

$$\begin{aligned} D_{j,n+1} &= D_{j,n+1}(x_{j,n+1}, y_{j,n+1}; x_{j,n}, u_{j|k}, \hat{d}_{j|k}) \\ &= x_{j,n+1} - F(y_{j,n+1}, u_{j|k}, \hat{d}_{j|k})\Delta t_{j,n} - x_{j,n}. \end{aligned} \tag{28}$$

Furthermore, $w_{j+1,0} = w_{j,N_j}$. We substitute the discretized DAEs (27) into (25) and approximate the integral in (24) with a right rectangle quadrature rule:

$$\psi = \psi(\{u_{j|k}\}_{j=k}^{k+N_h-1}; \hat{x}_{k|k}, \{\hat{d}_{j|k}\}_{j=k}^{k+N_h-1}) \tag{29a}$$

$$= \left\{ \phi = \sum_{j=k}^{k+N_h-1} \sum_{n=0}^{N_j-1} \Phi_{j,n}(y_{j,n+1}, u_{j|k}, \hat{d}_{j|k}) : \tag{29b}$$

$$x_{k,0} = \hat{x}_{k|k}, \tag{29c}$$

$$R_{j,n+1}(w_{j,n+1}; x_{j,n}, u_{j|k}, \hat{d}_{j|k}) = 0 \right\}. \tag{29d}$$

$n = 0, \ldots, N_j - 1$ and $j = k, \ldots, k+N_h-1$ in (29d) and

$$\Phi_{j,n}(y_{j,n+1}, u_{j|k}, \hat{d}_{j|k}) = \Phi(y_{j,n+1}, u_{j|k}, \hat{d}_{j|k})\Delta t_{j,n}. \tag{30}$$

Proposition 1. Consider the function, ψ, defined in (29). The gradients, $\nabla_{u_{j|k}}\psi$, can be computed by

$$\nabla_{u_{j|k}}\psi = \sum_{n=0}^{N_j-1} \left(\nabla_{u_{j|k}}\Phi_{j,n} + \left(\frac{\partial R_{j,n+1}}{\partial u_{j|k}} \right)' \lambda_{j,n+1} \right), \tag{31}$$

where the adjoints satisfy

$$\left(\frac{\partial R_{j,N_j}}{\partial w_{j,N_j}} \right)' \lambda_{j,N_j} = -\nabla_{w_{j,N_j}}\Phi_{j,N_j-1}, \tag{32}$$

for $j = k+N_h-1$,

$$\left(\frac{\partial R_{j,n}}{\partial w_{j,n}} \right)' \lambda_{j,n} = -\left(\frac{\partial R_{j,n+1}}{\partial w_{j,n}} \right)' \lambda_{j,n+1} - \nabla_{w_{j,n}}\Phi_{j,n-1}, \tag{33}$$

for $n = N_j - 1, \ldots, 1$ and $j = k+N_h-1, \ldots, k$, and

$$\begin{aligned} \left(\frac{\partial R_{j,N_j}}{\partial w_{j,N_j}} \right)' \lambda_{j,N_j} = &-\left(\frac{\partial R_{j+1,1}}{\partial w_{j+1,0}} \right)' \lambda_{j+1,1} \\ &- \nabla_{w_{j,N_j}}\Phi_{j,N_j-1}, \end{aligned} \tag{34}$$

for $j = k+N_h-2, \ldots, k$.

6. DYNAMIC UV FLASH SEPARATION

We consider the flash separation of a mixture of N_C components into a vapor phase (v) and a liquid phase (l). The two phases are in thermodynamic equilibrium. The vapor and liquid phases exit the separator from two separate streams. The separator is supplied with a vapor-liquid mixture through a feed stream. The separator is cooled, $Q(t) \leq 0$. The internal energy, U, and the total amount of moles of each component, n, are described by the conservation equations

$$\dot{U}(t) = H_F^v(t) + H_F^l(t) - H_V(t) - H_L(t) + Q(t), \tag{35a}$$

$$\dot{n}_i(t) = f_{F,i}^v(t) + f_{F,i}^l(t) - v_i(t) - l_i(t), \quad i = 1, \ldots, N_C. \tag{35b}$$

H_F^v and H_F^l are the vapor-liquid enthalpies of the feed stream, and H_V and H_L are the enthalpies of the vapor and liquid streams. Q is the heat flux from the external cooling. f_F^v and f_F^l are vectors of the molar flow rates of the feed stream, and v and l are vectors of the molar flow rates of the vapor and liquid streams. The volume, V, of the separator is fixed. The equilibrium temperature, T, pressure, P, and vapor-liquid compositions, n^v and n^l, are the solution to the UV flash optimization problem:

$$\max_{T,P,n^v,n^l} \quad S = S^v(T,P,n^v) + S^l(T,P,n^l), \tag{36a}$$

$$\text{s.t.} \quad U^v(T,P,n^v) + U^l(T,P,n^l) = U, \tag{36b}$$

$$V^v(T,P,n^v) + V^l(T,P,n^l) = V, \tag{36c}$$

$$n_i^v + n_i^l = n_i, \quad i = 1, \ldots, N_C. \tag{36d}$$

The UV flash optimization problem (36) is a mathematical statement of the second law of thermodynamics, i.e. the entropy of a closed system in equilibrium is maximal. That condition can be adapted to isothermal-isobaric (constant temperature-constant pressure) systems in which case it states that Gibbs energy, G, is minimal. That is the condition that determines the molar flow rates of the feed stream, f_F^v and f_F^l, based on the feed temperature, T_F, pressure, P_F, and total molar flow rates, f_F:

$$\min_{f_F^v, f_F^l} \quad G = G^v(T_F, P_F, f_F^v) + G^l(T_F, P_F, f_F^l), \tag{37a}$$

$$f_{F,i}^v + f_{F,i}^l = f_{F,i}, \quad i = 1, \ldots, N_C. \tag{37b}$$

(37) is called the PT flash optimization problem. The first-order optimality conditions of (36) constitute the algebraic equations (1a). We solve (35) and (36) simultaneously. However, we nest the solution of (37) into the evaluation of the right-hand side of (35). The properties in the right-hand side of the conservation equations (35) are uncertain, e.g. because of limited accuracy in the thermodynamic parameters. The differential equations (35) are therefore stochastic, and the process noise can be non-additive depending on how the uncertain parameters enter into the model equations (Kolås et al., 2009).

7. NUMERICAL EXAMPLE

We consider the flash separation of a hydrocarbon mixture in a 1 m^3 separator. The feed mixture contains 60% C_1, 10% C_2, 5% C_3, 23% n-C_7, and 2% H_2S. There are 6 states, 12 algebraic variables, and 7 adjoint algebraic variables. We control the separation process over a time period of 8 h. The prediction and control horizon in the NMPC algorithm is 6 h. The manipulated inputs are the heat flux, Q, and the total flow rates of the vapor and liquid streams, F_V and F_L. The total feed flow rate is $F_F = 12$ kmol/h. The objective of the NMPC algorithm is to minimize the amount of energy spent on cooling, i.e. to maximize $\int_{0\,\mathrm{h}}^{8\,\mathrm{h}} Q(t)dt$ (which is negative). There are upper bounds on the H_2S vapor mole fraction, $y_{H_2S} \leq 2\%$, and the pressure, $P \leq 7.5$ MPa. We incorporate those bounds into the objective function with logarithmic barrier functions. We incorporate bounds on the vapor fraction, $\beta \in [0\%, 100\%]$, in a similar manner. The feed temperature, T_F, is an unknown disturbance variable that we estimate. The initial estimate of T_F is equal to its true value. However, T_F increases with 5 K after 2 h. This increase is not known by the NMPC algorithm. We use $\sigma_d = 0.5$ K and $P_0^{dd} = 0.25^2$ K^2 in the EKF. We measure the temperature and pressure every 5 min. This is also the length of the control intervals. The standard deviations of the temperature and pressure measurement noises are 2.5 K and 0.05 MPa. The diffusion coefficient is constant, i.e. $\sigma(y(t), u(t), d(t)) = \sigma = \mathrm{diag}([\sigma_U; \sigma_{C_1}; \sigma_{C_2}; \sigma_{C_3}; \sigma_{\text{n-}C_7}; \sigma_{H_2S}])$ where $\sigma_U = 0.2$ MJ, $\sigma_{C_1} = \sigma_{C_2} = \sigma_{\text{n-}C_7} = 2$ mol, and $\sigma_{C_3} = \sigma_{H_2S} = 0.2$ mol. x_0 is a steady-state of the system (when process noise is disregarded), and $P_0^{xx} = \sigma\sigma'$.

Fig. 1 shows a closed-loop simulation of NMPC of the flash separation process. The upper bounds on y_{H_2S} and P are satisfied throughout the entire simulation. Fig. 2 shows the estimated disturbance variable, T_F, together with the manipulated inputs, Q, F_V, and F_L. The EKF is able to track the increase in T_F, and the NMPC algorithm is able to reduce the cooling and thereby lower the energy consumption. The computation time of the NMPC algorithm is between 0.21 s and 3.14 s in each of the control intervals, and the average computation time is 0.64 s.

8. CONCLUSIONS

We present an NMPC algorithm for disturbance rejection in isoenergetic-isochoric flash processes (also called UV flash processes). It estimates the states and the unknown disturbance variables with the continuous-discrete EKF and solves the involved OCPs with a single-shooting method. The gradients are computed with an adjoint method. It is natural for models of UV flash processes to be in a semi-explicit index-1 stochastic DAE form. We describe a model of a UV flash separation process in such a form. We present a numerical example of economical NMPC of the UV flash separation process. The example involves constraints on the H_2S vapor mole fraction and the pressure, and the estimation is based on temperature and pressure measurements. The NMPC algorithm is able to estimate an unknown increase in the unmeasured feed temperature while satisfying the constraints. The computation time is 3.14 s or less in all of the 5 min control intervals which indicates that real-time NMPC of UV flash processes is computationally feasible.

REFERENCES

Alessandri, A., Baglietto, M., Battistelli, G., and Zavala, V. (2010). Advances in moving horizon estimation for nonlinear systems. In *Proceedings of the 49th IEEE Conference on Decision and Control*. Atlanta, Georgia, USA.

Arendsen, A.R.J. and Versteeg, G.F. (2009). Dynamic thermodynamics with internal energy, volume, and amount of moles as states: application to liquefied gas tank. *Industrial & Engineering Chemistry Research*, 48(6), 3167–3176.

Binder, T., Blank, L., Bock, H.G., Bulirsch, R., Dahmen, W., Diehl, M., Kronseder, T., Marquardt, W., Schlöder, J.P., and von Stryk, O. (2001). Introduction to model based optimization of chemical processes on moving horizons. In *Online Optimization of Large Scale Systems*, 295–339. Springer-Verlag Berlin Heidelberg.

Castier, M. (2010). Dynamic simulation of fluids in vessels via entropy maximization. *Journal of Industrial and Engineering Chemistry*, 16(1), 122–129.

Evensen, G. (2009a). *Data assimilation: the ensemble Kalman filter*. Springer-Verlag Berlin Heidelberg, 2nd edition.

Evensen, G. (2009b). The ensemble Kalman filter for combined state and parameter estimation. *IEEE Control Systems Magazine*, 29(3), 83–104.

Flatby, P., Skogestad, S., and Lundström, P. (1994). Rigorous dynamic simulation of distillation columns based on UV-flash. *IFAC Proceedings Volumes*, 27(2), 261–266.

Hammer, M. and Morin, A. (2014). A method for simulating two-phase pipe flow with real equations of state. *Computers & Fluids*, 100, 45–58.

Huang, R., Biegler, L.T., and Patwardhan, S.C. (2010). Fast offset-free nonlinear model predictive control based on moving horizon estimation. *Industrial & Engineering Chemistry Research*, 49(17), 7882–7890.

Jørgensen, J.B. (2007). Adjoint sensitivity results for predictive control, state- and parameter-estimation with nonlinear models. In *Proceedings of the 2007 European Control Conference*, 3649–3656.

Jørgensen, J.B., Kristensen, M.R., Thomsen, P.G., and Madsen, H. (2007). New extended Kalman filter algorithms for stochastic differential algebraic equations. In *Assessment and Future Directions of Nonlinear Model Predictive Control*, volume 358 of *Lecture Notes in Con-*

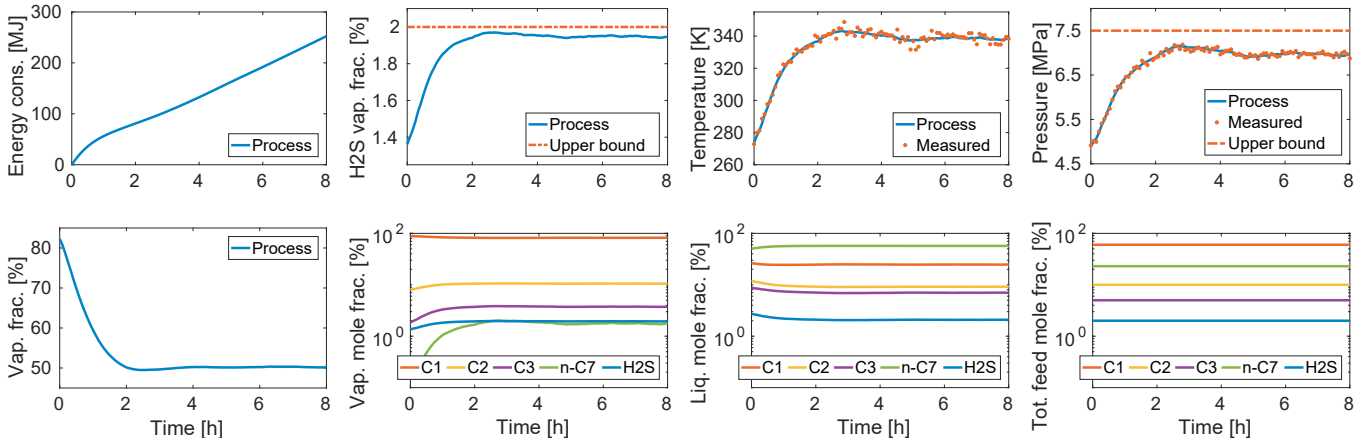

Fig. 1. Closed-loop simulation of the flash separation process. Top row: Energy consumption and H_2S vapor mole fraction as well as actual and measured temperature and pressure. Bottom row: Vapor fraction and vapor-liquid mole fractions of the mixture in the separator and total mole fractions of the feed.

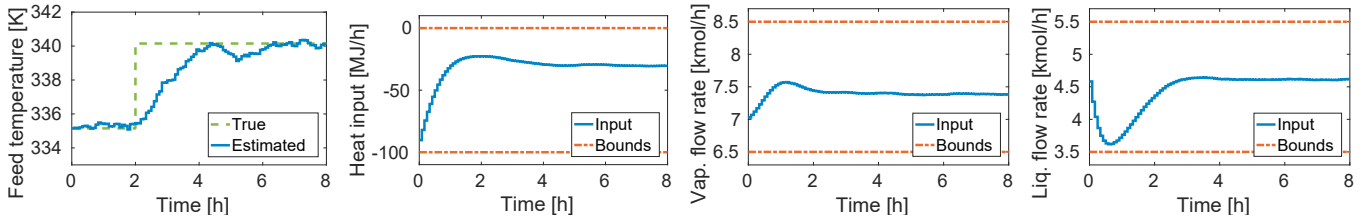

Fig. 2. The estimated disturbance variable, T_F, and the manipulated inputs, Q, F_V, and F_L.

trol and Information Sciences, 359–366. Springer-Verlag Berlin Heidelberg.

Kolås, S., Foss, B.A., and Schei, T.S. (2009). Noise modeling concepts in nonlinear state estimation. *Journal of Process Control*, 19(7), 1111–1125.

Kristensen, M.R., Jørgensen, J.B., Thomsen, P.G., and Jørgensen, S.B. (2004). An ESDIRK method with sensitivity analysis capabilities. *Computers & Chemical Engineering*, 28(12), 2695–2707.

Lima, E.R.A., Castier, M., and Biscaia Jr., E.C. (2008). Differential-algebraic approach to dynamic simulations of flash drums with rigorous evaluation of physical properties. *Oil & Gas Science and Technology – Rev. IFP*, 63(5), 677–686.

Michelsen, M.L. (1999). State function based flash specifications. *Fluid Phase Equilibria*, 158-160, 617–626.

Mobed, P., Munusamy, S., Bhattacharyya, D., and Rengaswamy, R. (2017). State and parameter estimation in distributed constrained systems. 1. extended Kalman filtering of a special class of differential-algebraic equation systems. *Industrial & Engineering Chemistry Research*, 56(1), 206–215.

Morari, M. and Maeder, U. (2012). Nonlinear offset-free model predictive control. *Automatica*, 48(9), 2059–2067.

Qiu, L., Wang, Y., and Reitz, R.D. (2014). Multiphase dynamic flash simulations using entropy maximization and application to compressible flow with phase change. *AIChE Journal*, 60(8), 3013–3024.

Ritschel, T.K.S., Capolei, A., Gaspar, J., and Jørgensen, J.B. (2018). An algorithm for gradient-based dynamic optimization of UV flash processes. *Computers and Chemical Engineering*, 114, 281–295.

Ritschel, T.K.S., Gaspar, J., and Jørgensen, J.B. (2017). A thermodynamic library for simulation and optimization of dynamic processes. *IFAC-PapersOnLine*, 50(1), 3542–3547.

Ritschel, T.K.S., Gaspar, J., Capolei, A., and Jørgensen, J.B. (2016). An open-source thermodynamic software library. Technical Report DTU Compute Technical Report-2016-12, Department of Applied Mathematics and Computer Science, Technical University of Denmark.

Ritschel, T.K.S. and Jørgensen, J.B. (2018). The extended Kalman filter for state estimation of dynamic UV flash processes. *IFAC-PapersOnLine*, 51(8), 164–169.

Simon, D. (2006). *Optimal state estimation: Kalman, H infinity, and nonlinear approaches*. John Wiley & Sons.

Subramanian, S., Lucia, S., and Engell, S. (2015). Handling structural plant-model mistmatch via multi-stage nonlinear model predictive control. In *Proceedings of the 2015 European Control Conference*, 1602–1607. Linz, Austria.

Talebi, H.A., Abdollahi, F., Patel, R.V., and Khorasani, K. (2010). *Neural network-based state estimation of nonlinear systems: application to fault detection and isolation*, volume 395 of *Lecture Notes in Control and Information Sciences*. Springer-Verlag New York.

Vatankhah, B. and Farrokhi, M. (2017). Nonlinear model-predictive control with disturbance rejection property using adaptive neural networks. *Journal of the Franklin Institute*, 354(13), 5201–5220.